

1
2
3
4
5
6

Original Research Article
**Warming Effect Reanalysis of Greenhouse
Gases and Clouds**

ABSTRACT

The author has reanalysed the warming effects of greenhouse (GH) gases utilising the latest HITRAN 2012 database and improved water continuum calculations in the spectral analysis tool. The contributions of GH gases in the GH effect in the all-sky conditions are found to be: H₂O 81 %, CO₂ 13 %, O₃ 4 %, CH₄ & N₂O 1 %, and clouds 1 %. Because the total absorption is already 93 % from the maximum in the altitude of 1.6 km, which is the average global cloud base, the GH gas impacts are almost the same in the clear and all-sky conditions. The impacts of clouds are based on the normal cloudiness changes between the clear and cloudy skies. The positive impact of clouds is analysed and it is based on the warming impact of clouds during the night-time. The warming impact of CO₂ is very nonlinear and it means that in the present climate the strength of H₂O is 11.8 times stronger than CO₂, when in the total GH effect this relationship is 6.2:1. The atmospheric Total Precipitable Water (TPW) changes during ENSO events are the essential parts of the ENSO process and they are not actually separate feedback processes. The TPW changes during the ENSO events almost double the original ENSO effects. On the other hand, during Mt. Pinatubo eruption and during the three latest solar cycles, the long-term water feedback effect cannot be found despite of rapid warming from 1980 to 2000. This empirical result confirms that the assumption of no water feedback in calculating the climate sensitivity of 0.6 °C is justified. Because there is no long-term positive feedback, it explains why the IPCC model calculated temperature 1.2 °C in 2015 is 44 % greater than the average 0.85 °C of the pause period since 2000.

7
8
9
10
11

Keywords: Global warming; greenhouse effect; greenhouse gases; climate sensitivity; cloud forcing; water feedback

12

13 **1. INTRODUCTION**

14

15 **1.1 Objectives and Symbols**

16

17 The physical properties of greenhouse (GH) gases in absorbing shortwave and longwave
 18 radiation have been well-known for decades. The latest updated knowledge has not been
 19 always available in some common spectral analysis tools. This has been also the case with
 20 the Spectral Calculator [1], the tool used by the author in earlier analyses. Now the latest
 21 HITRAN line data version 2012 is available [2]. The coefficients in water continuum model
 22 are also updated as to 2.5.2 MT_CK [3].

23

24 These updates created an objective to reanalyse the warming impacts of GH gases in the
 25 GH phenomenon itself and the real impacts in the present climate. The warming and cooling
 26 effects of clouds have been a continuous issue of different opinions and therefore it is
 27 another objective of this study. The third objective is to carry out a water feedback analysis,
 28 which has a major impact on the climate sensitivity (CS).

29

30 Table 1 includes all the symbols, abbreviations, acronyms, and definitions used repeatedly in
 31 this paper.

32

33 **Table 1. List of symbols, abbreviations, and acronyms**

34

Acronym	Definition
AGA	Average Global Atmosphere
CF	Cloud Forcing
CL	Cloudiness
CS	Climate Sensitivity
CSP	Climate Sensitivity Parameter ($=\lambda$)
ENSO	El Niño Southern Oscillation
GCM	General Circulation Model
LW	Longwave
MLS	Mid-latitude climate zone, summer
MLW	Mid-latitude climate zone, winter
OLR	Outgoing longwave radiation
prcm	precipitated water in centimetre
PS	Polar climate zone, summer
PW	Polar climate zone, winter
RF	Radiative Forcing change
SW	Shortwave
TCF	Temporary Climate Forcing
TOA	Top of the Atmosphere
TPW	Total Precipitable Water
TROP	Tropical climate zone
UAH	University of Alabama in Huntsville temperature data set

35

36

37 **1.2 The Survey of Greenhouse Effect Studies**

38

39 The difference between the average global mean surface temperature ($15\text{ }^{\circ}\text{C}$) and the
 40 temperature ($-19\text{ }^{\circ}\text{C}$) corresponding to the average outgoing longwave (LW) radiation (239
 41 Wm^2) at the top of the atmosphere (TOA) is a common measure of terrestrial GH effect thus

42 being 34 °C. The GH gases and clouds absorb the LW radiation emitted by the Earth's
43 surface and in this way, they prevent the cooling of the Earth making it a habitable planet.

44

45 The number of studies for calculating and analyzing the contributions of GH gases is
46 surprisingly low. The most important results are summarized in Table 2.

47

48 **Table 2. The contribution percentages of GH gases in the GH phenomenon after**
49 **different studies.**

50

GH gas	Michell	Kiehl & Trenberth	Schmidt et al.	Ollila
H ₂ O	65	60 (38)	50	82
CO ₂	32	26	19	11
O ₃	1	8	Others 7	5
CH ₄ & N ₂ O	2	6		2
Clouds		(39)	25	

51

52

53 Michell [4], Kiehl & Trenberth [5], and Ollila [6] have carried out the calculations in the clear
54 sky conditions and Schmidt et al (7) values are for all-sky. Kiehl & Trenberth have also two
55 percentages for cloudy sky conditions. In addition to these comprehensive studies, there are
56 some studies indicating percentages for individual GH gases: Clough et lacono [8] water 63
57 %, Miskolczi & Mlynczak [9] CO₂ 9 % and Pierrehumbert [10] CO₂ about 33 %.

58

59 The atmosphere composition applied in the calculations has a decisive role. Michell has not
60 specified the atmosphere. Kiehl & Trenberth have used US Standard 76 atmosphere (USST
61 76) and they have reduced the water content by 12 %. It means that in their analysis, the
62 water content is only 50 % about the average global atmosphere (AGA), which is 2.6 prcm
63 (precipitated water in centimeters). Ollila [11] has carried out these calculations also applying
64 the USST 76 and the results are very close to Kiehl & Trenberth [5]. Even though some
65 researchers [12] think that the use of USST 76 is an international and IPCC accepted
66 standard for atmospheric calculations, its composition makes it not applicable for any global
67 atmospheric calculations.

68

69 The calculation method is not similar in all studies. Kiehl & Trenberth [5], Miskolczi &
70 Mlynczak [9] and Ollila [11] have calculated the contribution of each GH gas by removing it
71 from the atmospheric model. Schmidt et al. [7] have used a more complicated method by
72 calculating the minimum and maximum impact. The minimum impact comes from the
73 removing process and the maximum by applying the GH gas in question alone in the
74 atmosphere. In this case, the result concerning the major absorbers water, carbon dioxide
75 and clouds is almost exactly the average value of minimum and maximum impacts.

76

77 Only Schmidt et al. [7] have proposed that clouds have a positive contribution in the GH
78 phenomenon even though they admit that the net radiative impact including SW effects of
79 clouds is one of cooling. This is one of the issues discussed and analyzed later in this study.

80

81 The spread of the results in the contributions of GH gas may have been a reason, why IPCC
82 has not concluded what are the most reliable values.

83

84 **1.3 Warming and Cooling Effects of Clouds**

85

86 Clouds have remained a subject of various and even opposite opinions in climate change
87 science. The term *cloud forcing* (CF) is commonly used. This effect is due to the difference

88 between the clear sky and all-sky conditions. The all-sky is the normal overall condition of
 89 the global atmosphere, where the average cloudiness is about 66 % [13]. The CF is
 90 specified as the difference between incoming SW radiation flux and outgoing LW radiation
 91 flux between clear sky and all-sky at TOA. The difference of SW radiation in these conditions
 92 is 51.2 Wm^{-2} , and the difference in LW radiation is 21.2 Wm^{-2} using the values of the study of
 93 Ollila [14]. In this study the major source of radiation fluxes are from Zhang et al. [15]. This
 94 means the CF value of -30.0 Wm^{-2} , which is cooling. A survey of the CF studies [14] shows
 95 that CF varies normally between the -17 Wm^{-2} and -28 Wm^{-2} giving the average value of $-$
 96 23.4 Wm^{-2} .

97
 98 It should be noticed that this specification has a special nature. The SW radiation change
 99 happens immediately, if the cloudiness changes. The LW radiation fluxes react immediately
 100 for cloudiness changes but SW changes start to warm up the atmosphere, the surface of the
 101 ocean and the land and it takes a long time before a new balance could be reached. The
 102 time constant is for ocean is 56 ± 11 days, 29 ± 6 days for the land [16], and 2.7 days for the
 103 atmosphere [14]. This means that in about one year the surface temperature would be close
 104 to the value corresponding to a new cloudiness value.

105
 106 In two studies the CF effect has been found to be $-0.11^\circ\text{C}/\text{CL}\%$ [17] and $-0.1^\circ\text{C}/\text{CL}\%$ [14],
 107 which are based on different research methods (CL-% = Cloudiness-%). This result means
 108 that the long-term cloudiness changes can result in relatively great temperature changes.
 109 For example, the permanent cloudiness change of 8 % would cause the temperature
 110 increase of 0.8°C .

111
 112 There is a special dynamic feature included in the CF phenomenon. It is not generally known
 113 or understood. It could be called *transient cloud forcing* (TCF). This phenomenon comes out
 114 in analyzing the radiative balance of the Earth's surface. This energy balance includes only
 115 two major incoming radiative fluxes: the SW flux from the Sun and the downward LW flux
 116 emitted by the atmosphere – sometimes called a reradiated LW flux. In calculating the final
 117 incoming SW flux on the surface, six different fluxes must be subtracted from the original
 118 insolation flux of the Sun.

119
 120 Ollila has carried out the calculation of the energy balance for clear, cloudy, and all-sky
 121 conditions [14], [18]. The summary of the balance for the surface is in Table 3.

122
 123 **Table 3. The energy budget of the Earth's surface. Clear and cloudy sky values are for**
 124 **pseudo-balance conditions.**
 125

Radiation flux, Wm^{-2}	Clear	Cloudy	All-sky
SW radiation absorbed by surface	190.0	154.8	166.8
Downward radiation emitted by atmosphere	318.0	359.0	344.7
Surface balance	508.0	513.8	511.8

126
 127 The balance values are very close to each other. The cloudy sky value is greater than the
 128 clear sky value. This seems to be incorrect, because the CF studies show that more clouds
 129 mean lower temperatures.

130
 131 The explanation is in the measurement time and in the dynamics of the cloudiness change.
 132 The Earth will never be in the steady-state conditions for clear and cloudy skies. Locally
 133 cloudiness changes continuously. For example, a measurement value of a clear sky means
 134 that the sky has been clear during some hours or days and in some rare cases even weeks.

135 It has not had time enough to reach the new steady state value of the clear sky, which
136 means that the surface is in the state of a dynamic change. Ollila [18] calls this state a
137 pseudo-balance state.
138

139 There is no reliable information available, that could be the average periods of clear and
140 cloudy skies locally in the global scale. A practical estimate could be 1 day for clear sky and
141 2 days for cloudy sky making the average cloudiness-% to be $100 \cdot 2/3 = 67\%$.
142

143 Why is the balance value of the cloudy sky greater than that of the clear sky? An analysis
144 shows, what happens, when the clear sky turns to the cloudy sky. In two or ten days, the
145 temperature of the surface ocean (70 % of the Earth's surface) does not decrease practically
146 at all regardless of radiation changes. The land surface temperature and especially the
147 temperature of the atmosphere start to change but they do not decrease but they increase.
148 The decrease effect will come later. This is called an inverse response and it is rather rare in
149 the process dynamics. The reason is in the diurnal radiation fluxes. The clouds trap more
150 LW radiation than the cloudless atmosphere and because of this, the downward radiation
151 increases from 318 Wm^{-2} to 359 Wm^{-2} , which is 5.8 Wm^{-2} more than the decrease of the SW
152 radiation from 190 Wm^{-2} to 154.8 Wm^{-2} .
153

154 The measured radiation fluxes [14] reveal that the radiation flux emitted by the surface is in
155 clear sky 394.1 Wm^{-2} , and in cloudy sky 396.3 Wm^{-2} . They correspond the black surface
156 temperatures of $15.6 \text{ }^{\circ}\text{C}$ and $16.0 \text{ }^{\circ}\text{C}$, which is in line with the surface balance values. These
157 are the effects of the TCF phenomenon. Because the incoming SW radiation is the original
158 energy source of the Earth, the surface temperature must follow the decreasing SW
159 radiation flux eventually. The downward radiation flux depends on the incoming radiation flux
160 directly (= SW radiation absorption by the atmosphere) and indirectly (= the GH gases
161 absorb LW radiation emitted the surface) and it must decrease later according to the time
162 constants of the ocean, land and the atmosphere.
163

164 What is the time, when the temperature reacts into "wrong" direction? In this example the
165 temperature increases first 0.4 degrees and thereafter it starts gradually to decrease
166 depending mainly on the time constant of the atmosphere, which is 2.7 days. The time
167 needed to overcome this "wrong" direction change is from 2 to 10 days. TCF is a real
168 phenomenon, which has been confirmed by the radiation flux measurements. Even though
169 TCF reacts firstly in the "wrong" direction, it should not be confused with the temperature
170 change of CF. CF and TCF phenomena have critical roles in calculating the contributions of
171 clouds in the GH effect.
172

173 **2. ABSORPTION BY GREENHOUSE GASES**

174 **2.1 Effects of HITRAN 2012 and Water Continuum**

175 The first calculations were carried out to find out the impacts of HITRAN 2012 and water
176 continuum updates in the absorption calculations. The author has used in earlier studies the
177 atmospheric one profile model called average global atmosphere (AGA) [6], [11], [14], [18],
178 [19], [20]. This model was based on the GH gas concentrations in 2005 and therefore it is
179 called AGA05. The GH gas concentrations of AGA05 are modified from the GH gas profiles
180 of the Polar Summer of Spectral Calculator to correspond the values reported by IPCC [21].
181 The water profile was adjusted in such a way that the total precipitable water (TPW) was 2.6
182 cm [22].
183

184
185
186 The total absorption in the troposphere applying the AGA05 condition and the HITRAN 2008
187 version was 302.709 Wm^{-2} . When the AGA05 was applied using the newest HITRAN 2012

188 version and the updated water continuum, the total absorption was 303.308 Wm^{-2} . It is only
 189 a 0.2 % greater value, which mean that these updates have a very small effect for
 190 absorption calculations.

191

192 In later calculations of this study, the GH gas concentrations are updated to correspond with
 193 the values in year 2015 [23] and therefore this climate model is called AGA15. The AGA15
 194 profile gives the value of 305.978 Wm^{-2} as the total absorption. The difference is mainly due
 195 to the higher CO_2 concentration (400.83 ppm versus 379 ppm).

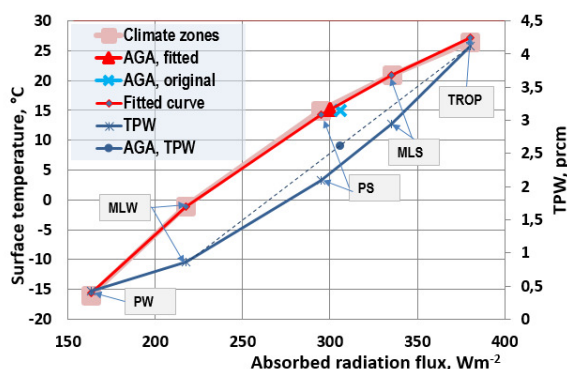
196

197 **2.2 Simulation of Climate Zones**

198

199 I have used one climate profile in calculations utilizing AGA15. Because the climate varies in
 200 the different climate zones, the question is, how well one profile represents the global
 201 conditions. This can be tested by calculating the absorption in the troposphere applying 5
 202 climate zones: tropical (TROP), mid-latitude summer (MLS), mid-latitude winter (MLW), polar
 203 summer (PS) and polar winter (PW). The results of these calculations are (Wm^{-2}): PW
 204 163.329, PS 294.701, MLW 217.534, MLS 335.221, and TROP 380.064. Utilizing the
 205 weighting factor based on the geographical areas for these climate zones [19], the global
 206 absorption value is 307.533 Wm^{-2} . It is only 0.5 % higher than 305.978 Wm^{-2} calculated
 207 applying the one profile approach AGA15. The difference is mainly due to the fact that the
 208 TPW value of climate zones is 2.7 cm and the one of AGA15 is 2.6 cm. The results of these
 209 calculations are depicted in Figure 1.

210



211

212

213

214

215

216

217

Figure 1. The relationship between the absorption fluxes, temperatures, and water contents of different climate zones. The climate zones of the curves starting from the left corner are PW, MLW, PS, MLS, TROP. The temperatures and TPW values are from the climate profiles of Spectral Calculator [1].

218

219

220

221

222

223

224

225

226

227

228

229

The relationship between the temperatures ($T, ^\circ\text{C}$) and absorption energies (E, Wm^{-2}) is logarithmic:

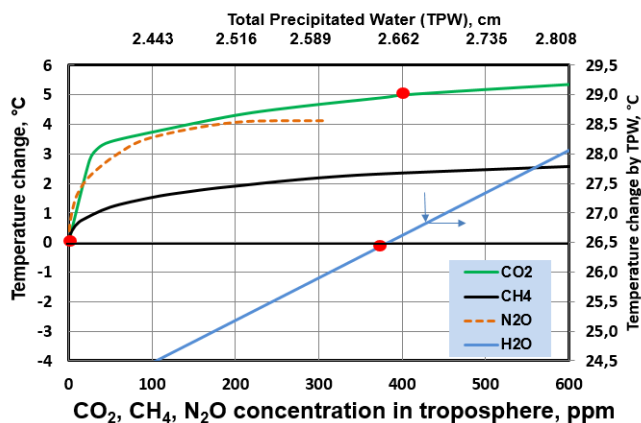
$$T = -274.3249 + 50.7558 * \ln(E) \quad (1)$$

The coefficient of determination r^2 is 0.999 and the standard error of the temperature estimate is $0.9 ^\circ\text{C}$. In Fig.1 is depicted also the AGA15 value, which is $15 ^\circ\text{C} / 305.978 \text{ Wm}^{-2}$. This point is not exactly on the fitting curve, because the overall TPW value of climate zones is 2.7 cm and the one of AGA15 is 2.6 cm. The AGA15 point (a blue cross) is slightly modified to fit it (a red triangle) on the curve applying the values of $15.19 ^\circ\text{C} / 300 \text{ Wm}^{-2}$. The blue curve shows the increasing TPW values according to the warmer climate zones. The blue dot is the AGA15 value of 2.6 prcm.

230 **2.3 Warming Impacts of Greenhouse Gases in the Clear Sky**

231
232
233
234
235
236

Applying the AGA15 atmospheric profile, the absorption values of GH gases can be calculated by changing the concentration of each GH gas starting from zero level in clear sky condition. The warming effects can be then calculated by using equation (1). The results are depicted in Fig. 2.



237
238
239
240

Fig. 2. The warming impacts of GH gases in the clear sky conditions. The red dots represent the concentrations and warming impacts of the year 2015.

241 The warming effect of CO₂ is highly nonlinear in the present atmosphere but the effect of
242 H₂O is practically linear around the average TPW value of 2.6 cm. Also, the concentrations
243 of CH₄ and N₂O are so low that they are still in the region of Beer-Lambert law, where the
244 absorption is almost linearly dependent on the gas concentration. The warming impacts of
245 CO₂ can be fitted with the logarithmic equation:

246

$$T = -1.01403 + 0.988487 * \ln(CO_2) \quad (2)$$

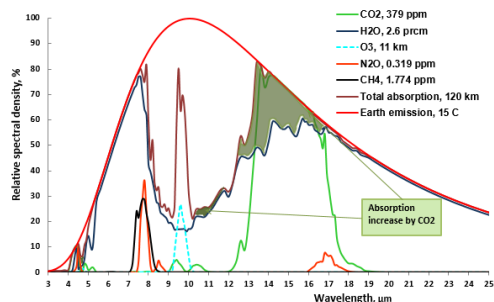
247

248 where T is the temperature impact (°C) and CO₂ is the concentration of CO₂ (ppm). The
249 coefficient of determination r² is 0.999, the standard error is 0.02 °C. This formula is valid in
250 the concentration range from 200 ppm to 800 ppm. This formula gives the temperature
251 change 0.6 °C for the CO₂ concentration from 280 ppm to 560 ppm.

252

253 The reasons for the nonlinear effects can be illustrated by the absorption graphs of GH
254 gases, when the relative spectral density is calculated as a function of wavelength. In Fig. 3
255 the absorption graphs are depicted from the 3 μm to 25 μm.

256



257
258
259
260

Figure 3. The absorption band Graphs of GH gases in the AGA05 atmosphere. The green shaded areas indicate a total warming impact of CO₂ of concentration of 379 ppm.

261
262 Water absorbs completely all the IR radiation emitted by the Earth's surface in the
263 wavelength zone from 25 μm to 100 μm . The shaded green area gives a good image of the
264 magnitude of CO_2 . The absorption area changes due to the increased concentrations of
265 CO_2 , CH_4 , and N_2O from 2005 to 2015 are so small that they could not be detected in the
266 graphical presentation of Fig. 3.

267
268 The curve of each GH gas is calculated when it is the only GH gas in the atmosphere in the
269 AGA05 conditions. The combined effect of all GH gases is not a summary of the band areas
270 of single GH gases. The actual total absorption can be calculated only when all the GH
271 gases are present at the same time. The total absorption is depicted by the purple line. The
272 absorption areas of CH_4 and N_2O show that they are very small and inside the absorption
273 areas of H_2O , which reduces their impacts further. Also, the CO_2 absorption area overlaps
274 with water and the real impacts are possible to calculate only by the means of spectral
275 analysis by varying the CO_2 concentration.

276

277 **3. WATER FEEDBACK**

278

279 **3.1 Water Feedback in the Climate Zones**

280

281 Water feedback is one of the most important issues in the climate change science. The
282 results and opinion deviate completely from each other. IPCC and many research
283 communities use the approach that water feedback exists and it is positive in nature by
284 doubling the warming effects of other GH gases. The Table 9.5 in AR5 [24] summarizes 30
285 different GCMs (General Circulation Model), which have the Climate Sensitivity Parameter
286 (CSP or λ) averaging 1.0 $\text{K}/(\text{Wm}^2)$. Because this CSP value is for Equilibrium Climate
287 Sensitivity (ECS) value, it includes water feedback and other positive feedbacks. The CSP
288 value of 0.5 $\text{K}/(\text{Wm}^2)$ includes only water feedback [24]. The opposite result is from
289 Miskolczi [22] that the GH effect of the Earth's climate is constant, which means that the
290 water feedback is negatively compensating for the warming effects of other GH gases.

291

292 One possible way to analyze the water feedback is to calculate the warming effect of water
293 by hypothesizing that the Earth's climate follows the humidity features of the climate zones.
294 From Fig. 1 it is easy to find out that the absolute water content increases as the climate is
295 getting warmer.

296

297 The absorption flux of CO_2 concentration 280 ppm is 298.728 Wm^{-2} and the same of CO_2
298 concentration 560 ppm is 301.177 Wm^{-2} , which corresponds the temperature change of 0.48
299 $^\circ\text{C}$ according to equation (1). If we assume that the absolute water content of the global
300 atmosphere follows the climate zone behavior, the water content change would increase this
301 absorption change like this: 280 ppm absorption 297.728 Wm^2 and 560 ppm absorption
302 301.592 Wm^{-2} . This change corresponds to the temperature change 0.66 $^\circ\text{C}$. Thus, the
303 water feedback would positively increase the warming effects of GH gases by 35.4 %.

304

305 **3.2 Water Feedback During the Last 25 Years**

306

307 Rather reliable conclusions about the water feedback can be drawn from the behavior of the
308 climate during the last 35 years. I have selected this period, because the encompassing
309 satellite temperature measurements were introduced in 1979. Also, a new humidity
310 semiconductor sensor technology Humicap® was introduced by the leading humidity
311 measurement company Vaisala. This technology replaced rapidly the hygrometer
312 technology, because it was more accurate and more reliable than the hygrometer
313 technology.

314

315 I have started the analysis from the year 1979 by modifying temperature changes and all
 316 warming impacts to start from zero. The temperature is according to the UAH satellite data
 317 set [25] and absolute TPW values from NOAA [26] NCEP/NCAR Reanalysis dataset. The
 318 warming impacts of water are calculated based on the absorption calculations by increasing
 319 the water content of the AGA conditions (2.6 prcm / 305.978 Wm⁻²) to the TPW value of
 320 2.856 prcm giving the absorption value of 306.709 Wm⁻². By forcing the warming value (T)
 321 in Celcius degrees to be zero in 1979, equation (3) could be concluded:

322

$$T = -6.797 + 2.81 * TPW, \quad (3)$$

324

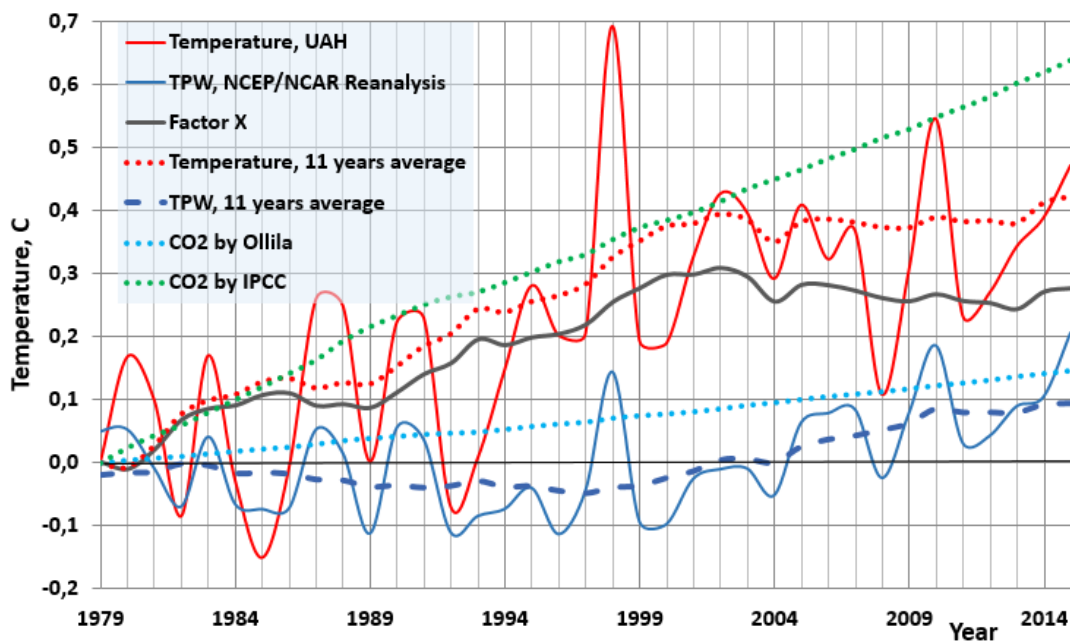
325 where TPW is the absolute humidity in prcm. The warming impact of CO₂ is calculated by
 326 the equation introduced by Ollila [6]:

327

$$T = CSP * k * \ln(C/280), \quad (4)$$

329

330 where CSP is 0.27 K/(Wm⁻², and k is 3.12 in the formula of radiative forcing of CO₂ (Wm⁻²).
 331 The CO₂ concentration changes are from the data set of NOAA [23]. The results of these
 332 calculations are depicted in Fig. 4.



333

334

335

336

337

338

339

340

Figure 4. The temperature trend from according to UAH [25] and the major warming factors, which are absolute humidity and CO₂. The variable labelled “Factor” is the difference between the measured average temperature and the warming impacts of CO₂ by Ollila [6]. El Niño events are marked as to the strengths and they are followed by La Niña events which are not marked.

341

342

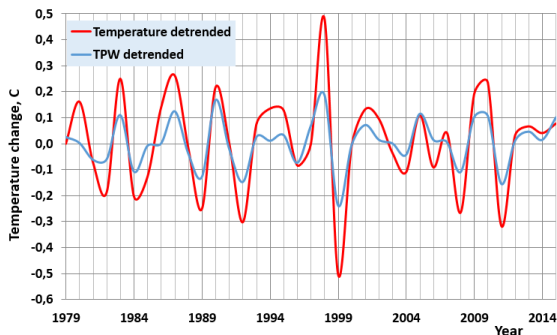
343

344

345

The variable labelled “Factor X” is also depicted in Fig. 4. It is the difference between the measured average 11 years temperature and the warming effect of CO₂ by Ollila [6]. This presentation makes it very clear that the warming impacts of water, CO₂, and ENSO events cannot explain the observed warming. It is easy to notice that the short-term temperature changes very closely correlated to the TPW changes. This relationship is even easier to

346 notice from Fig. 5, where these two variables are detrended. All the short-term changes are
 347 ENSO events except Mt. Pinatubo eruption in 1991.
 348



349 **Figure 5. The detrended graphs of temperature and TPW values.**

350
 351
 352 A hasty conclusion would be that the TPW variations have caused the temperature changes
 353 since 1979 until today. Looking at the shape of the monotonically rising temperature effect of
 354 CO₂ (IPCC or Ollila) and the sharp short-term changes of TPW, it is very clear that the
 355 relationship between these two variables is very poor.
 356

357 The detrended analysis reveals that the short-term TPW changes could explain about 50 %
 358 of the short-term temperature changes. Concerning the El Niño / La Niña events, we already
 359 know that the cause is the regional changes in Pacific Ocean currents and winds. They
 360 initiate the temperature change and the strong change of TPW amplifies the change by a
 361 factor of about 100 percent. It is practically the same as the positive feedback used by IPCC,
 362 but can it be found in the long-term trends?
 363

364 There is an essential feature in the long-term trends of temperature and TPW, which are
 365 calculated and depicted as 11 years running mean values. The long-term value of
 366 temperature has increased about 0.4 °C since 1979 and it has now paused to this level. The
 367 long-term trend of TPW shows a minor decrease of 0.05 °C during the temperature
 368 increasing period from 1979 to 2000 and thereafter only a small increase of 0.08 °C during
 369 the present temperature pause period. It means that the absolute water amount of the
 370 atmosphere is practically constant reacting only very slightly to the long-term trends of
 371 temperature changes. Long-term changes, which last at least one solar cycle (from 10.5 to
 372 13.5 years), are the shortest period to be analyzed in the climate change science. The
 373 assumption that the relative humidity is constant and it amplifies the GH gas changes by
 374 doubling the warming effects, finds no grounds based on the behavior of TWP trend.
 375

376 It seems that there is a dilemma between the short-term behavior of TPW changes and the
 377 long-term (> 11 years) changes. It looks like that the global atmosphere does not behave in
 378 the same way as it does in the climate zones, where a higher temperature means always a
 379 higher TWP value. Because the analysis period is slightly more than three solar cycles, the
 380 conclusions for long-term behavior of TPW is rather reliable. This result supports the climate
 381 sensitivity (CS) calculations, where the absolute water amount has been assumed to be
 382 constant, and which gives the CS value of 0.6 °C [6].
 383

384 So, there is a “Factor X”, the unknown force or forces that change the Earth’s temperature.
 385 During the period from 1995 to 2005 these forces have caused a temperature increase of a
 386 0.2-0.3 °C and now these effects are decreasing, see the black curve in Fig. 4. These forces
 387 are outside of the scope of this study but they could be the cosmic forces such as the Sun
 388 and other forces acting in our solar system. There are studies proposing the possible

389 reasons [27], [28] and the synthesis analysis combining these reasons together with the GH
390 gases [29] showing very high correlations starting from year 1880.

391

392 In Fig. 4 is also depicted the warming impact of GH gases according to the IPCC. This graph
393 is calculated using the CSP value of $0.5 \text{ K}/(\text{Wm}^{-2})$ and the radiative forcing (RF) values of
394 GH gases. The temperature change, according to this method, is about $0.2 \text{ }^{\circ}\text{C}$ higher than
395 the measured temperature at the end of the period. The error becomes even greater, if the
396 calculation would be started from the year 1750. The RF of GH gases in 2011 was 2.29
397 Wm^{-2} [24] and the increase from 2011 to 2015 has been 0.149 Wm^{-2} [30]. This means that
398 the temperature increase caused by GH gases would be $0.5 \text{ (K}/(\text{Wm}^{-2})) * 2.44 \text{ Wm}^{-2} = 1.22$
399 $^{\circ}\text{C}$ since 1750. It is 44 % higher than $0.85 \text{ }^{\circ}\text{C}$ which is the average temperature of the pause
400 period since 2000.

401

402 During the period from 1979 to 2000 the IPCC-model follows very accurately the long-term
403 trend of temperature. Even during this period there is a serious problem in the model that it
404 is based on the positive feedback of water. During this period the real TWP content has a
405 slight downward trend, and therefore it cannot double the warming impacts of GH gases.
406 When the real causes of warming do not increase anymore after 2000, the IPCC model still
407 shows a strong increasing trend.

408

409 **4. CONTRIBUTIONS OF GREENHOUSE GASES IN GLOBAL WARMING**

410

411 **4.1 The Contributions of Greenhouse Gases in the Greenhouse Effect**

412

413 As summarized in section 1.2, the results of GH gases in the GH effects deviate a lot in the
414 published research results. Because the lowest values for CO_2 warming effects are
415 calculated for clear sky conditions, I have carried out a new analysis for calculating the
416 results for all-sky conditions. The all-sky radiation fluxes and temperatures can be calculated
417 as a combination of clear and cloudy sky values [31] utilizing the following equation

418

$$419 \quad (1-k) * F_b + k * F_o = F_a \quad (5)$$

420

421 where F_b is the radiation flux of the clear sky, F_o is the radiation flux of the cloudy sky, F_a is
422 the radiation flux of the all-sky, and k is the all-sky cloud cover factor [18]. In this study the
423 value of k is 0.66, which means a cloudiness-% of 66 %.

424

425 The published values of average global cloud base and cloud top vary a lot. The results
426 based on the radiosonde stations are 0.6 km for the base and 9.0 km for the top in 1995
427 [32]. The same values based on the weather satellite measurements over 20 years' dataset
428 show the values of 1.6 km and 4.0 km [33]. The result of applying a semi-analytical cloud top
429 height retrieval algorithm based on an asymptotic solution of the radiative transfer equation
430 in the oxygen A-band gives the cloud top value of 6 km [34]. This analysis is valid for thick
431 clouds only.

432

433 In this study the cloud base and top values of 1.6 km and 4.0 km have been used. The
434 absorption calculations have been carried out by applying the AGA15 climate profile for the
435 altitude of 120 km. In this connection, the absorption according to the altitude was
436 calculated, and a technical problem in the Spectral Calculator was noticed. Namely the
437 absolute absorption change in 1 km altitude without CO_2 was 20.092 Wm^{-2} , and in the
438 altitude of 11 km, it was 16.515 Wm^{-2} . There are two probable reasons for this, which occur
439 at the same time.

440

441 In the atmospheric paths, the Spectral Calculator [1] divides the path into concentric
 442 spherical shells. The number of shells depends on the path and altitude range. For example,
 443 a path to 120 km altitude is split into 19 shells. The lowest shell is 250 meters thick and the
 444 highest is 10 km thick. In these shells, Spectral Calculator uses mass weighted values of
 445 temperature, pressure, and concentrations. This means that the calculation is more accurate
 446 for low altitude range of 1 km (the minimum for atmospheric paths) than the one of 11km
 447 range. This seems to create an accuracy problem for CO₂, which is a very strong GH gas in
 448 its absorption range from 12 μm to 19 μm. In the range from 14 μm to 16 μm CO₂ alone
 449 could easily absorb all the available infrared radiation emitted by the Earth's surface. In other
 450 words, in the presence of water, the CO₂ effect does not grow after the altitude of 1 km even
 451 though its concentration is practically the same up to the altitude of 80 km. After finding out
 452 this problem, the author has used the value of 20.092 Wm⁻² for the total contribution of CO₂
 453 from the concentration 0 ppm to 400.83 ppm. The author checked that this problem does not
 454 exist for CH₄ and N₂O, which are much weaker absorbers in the present-day atmosphere.
 455

456 A very decisive selection is the calculation method. I have calculated the contribution of each
 457 GH gas by removing it from the atmospheric model. One of the most essential features of
 458 our planet is the ocean covers 70 % of our planet's area. They provide humidity into the
 459 atmosphere, which has the key role in the GH phenomenon. Therefore, it is a justified
 460 assumption that there is water all the time in the atmosphere.
 461

462 The contributions are calculated for the clear sky and they are depicted in Table 4.
 463

464 **Table 4. The warming effects of GH gases in the clear sky conditions.**
 465

GH gas	Absorption	Absorption change	Percentage
Total	310.69		
CO ₂	294.25	20.1	14.9
O ₃	303.50	7.2	5.3
CH ₄ & N ₂ O	308.65	2.1	1.5
H ₂ O		105.7	78.3
Total		135.1	100.0

466 The total absorption of the clear sky 135.1 Wm⁻² is the difference of the surface emitted
 467 radiation flux 394.10 Wm⁻² and the OLR at the TOA 259 Wm⁻² [15]. These results show
 468 higher contribution for CO₂ (14.9 % versus 11.0 %) than those of the earlier study [6]. The
 469 contribution-% 14.9 is close to the one reported by Schmidt et al. [7] for a single factor
 470 removal process (14.0 %).
 471

472 The results for the cloudy sky are summarized in Table 5.
 473
 474

475
476
477
478

Table 5. The warming effects of GH gases in the cloudy sky conditions.

GH gas	Below clouds 0-1.6 km			Altitude 0-4.0 km		4-120 km	Cloudy sky, total	
	Absor.	Absor. change	%	Absor.	Absor. change	Absor. change	Absor. change	%
Total	289.03	21.66		301.75	22.36	8.94		
CO ₂	257.77	20.09	17.7	287.60	20.09	0.0	20.09	11.9
O ₃	277.64	0.33	0.3	301.02	0.73	6.46	6.79	4.0
CH ₄ & N ₂ O	276.73	1.32	1.1	300.21	1.54	0.51	1.74	1.0
H ₂ O		91.78	80.9		103.80	1.97	93.75	55.3
Clouds		0.0	0.0		0.0	0.0	47.02	27.8
Total		113.44	100		126.2		169.4	100

479
480
481
482
483
484
485
486
487
488
489
490
491
492
493
494

The total absorption 169.4 Wm^{-2} of the cloudy sky is the difference of the surface emitted radiation flux 396.20 Wm^{-2} and the OLR at the TOA 222.8 Wm^{-2} [15]. The absorption fluxes for the altitudes from the surface to 1.6 km and to 4.0 km, are calculated in the clear sky conditions. The absorption values for the altitude from 4 km to 120 km are calculated by subtracting the altitude 0-4 km values from the total absorption 0-120 km. The total GH gas absorption values can be calculated by summarizing the values of altitudes 0-1.6 km and 4-120 km. The difference of the total absorption 169.4 Wm^{-2} and the GH gases is 47.02 Wm^{-2} and it represents the absorption of clouds. It means that the contribution of clouds would be 27.8 %, which is close to 25 % which was reported by Schmidt et al. [7].

The absorptions and contributions of GH gases in all-sky conditions are summarized in Table 6.

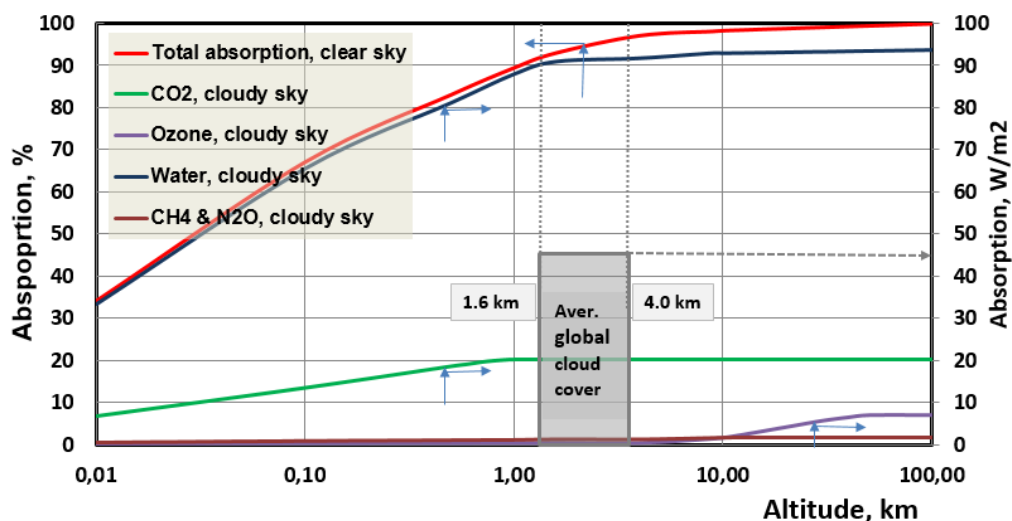
Table 6. The warming effects of GH gases in the all-sky conditions.

GH gas	All-sky, gross		All-sky, net		
	Absorp. change	%	Absorp. change	%	°C
CO ₂	20.1	12.7	20.1	12.7	4.3
O ₃	6.9	4.4	6.9	4.4	1.5
CH ₄ & N ₂ O	1.8	1.2	1.8	1.2	0.4
H ₂ O	97.8	62.0	127.3	80.7	27.4
Clouds	31.0	19.7	1.6	1.0	0.3
Total	157.7	100	157.7	100	34.0

495
496
497
498
499
500
501
502
503
504
505
506
507

The absorption flux values of the all-sky conditions are calculated using equation (5) and the values of clear and cloudy skies in Tables 4 and 5. The total absorption by GH gases and clouds in all-sky is 157.7 Wm^{-2} . The flux values representing the maximum effects of clouds, have been called *gross values*. Clouds decrease the incoming SW solar radiation but in this calculation basis it has not been considered. We can demonstrate this situation by the greenhouse having glass walls and roofs, and which locates in the polar zone in April. During day-time the incoming solar insolation decreases considerably the need for heating the greenhouse by gas or oil. At night-time, the solar insolation effect decreases and much more heating is needed and it may override the energy-savings at the day-time. If we would calculate the energy savings only during the day-time, we would draw a wrong conclusion that more glass in the walls and in the roof, means more energy savings.

508 That is the case of gross effect of clouds in Table 6. Therefore, there is also the *net effect*
 509 of clouds included in Table 6. The net effect of clouds is the combination of increased
 510 absorption by clouds and therefore increased LW flux downwards and the decreased SW
 511 radiation. The most reliable measure of this TCF effect is the observed surface temperature
 512 increase of 0.3 °C between clear sky and all-sky [15]. The increased absorption value of 1.6
 513 Wm^{-2} is a theoretical absorption increase, which could create this temperature change. The
 514 net absorption percentages of GH gases and clouds are calculated from the total absorption
 515 of 157.7 Wm^{-2} . This calculation basis is not univocal for H_2O , because it is calculated by
 516 subtracting the total absorption of other GH gases from the total absorption. Anyway, if the
 517 contribution-% of H_2O in the clear sky is 78.3 %, and the one of the all-sky is 80.7 %, the
 518 conclusion is that this small increase is in the right direction, because the humidity of the all-
 519 sky is higher than that of the clear sky. These results are depicted in Fig. 6.
 520
 521



522
 523 **Figure 6. The absorption effects of GH gases in the clear and cloudy sky conditions.**
 524
 525 The graphs in Fig.6 show that the total absorption in 1.6 km is already 93 % of that of 120
 526 km. That is why the GH impacts of all-sky are very close to the values of the clear sky. The
 527 absorption effects of O_3 happens mainly in the stratosphere.
 528

529 **4.2 The Relative Strengths**

530
 531 The analysis of the contributions of GH gases in the GH effect is not applicable for the
 532 present-day atmosphere. The reason is that the warming impacts are too nonlinear. A
 533 separate analysis was carried out to find out the relative strengths by increasing the
 534 concentrations by 10 % and calculating the absorption for the altitude of 120 km.
 535

536 Also in calculating the increased absorption caused by 10 % concentration increase, the
 537 CO_2 calculation was carried for the altitude of 1 km only. The other calculations were carried
 538 in the altitude of 120 km. The results are shown in Table 7.
 539

540 **Table 7. The increased absorption caused by the 10 % increase of concentration in**
 541 **AGA15 atmosphere. The reference value of the AGA15 absorption is 310.69 Wm⁻². The**
 542 **CO₂ change is based in the altitude of 1 km.**
 543

GH gas	Total absorption	Absorption change	Relative strength
H2O	315.129	4.439	11.765
CO2	(310.996)	0.394*	1
O3	310.998	0.308	0.782
N2O	310.745	0.055	0.140
CH4	310.733	0.043	0.109

544

545

546 In the earlier study the relationship between H₂O:CO₂ was 15.2:1 and now it is 11.8:1. The
 547 main reason is in the more accurate calculation method for CO₂ absorption.

548

549 **4. CONCLUSION**

550

551 The new updates of Spectral Calculator with HITRAN 2012 and water continuum increases
 552 the absorption results of GH gases in the atmosphere only by 0.2 % in comparison to the
 553 older versions. This means that the results using the older versions are still applicable.

554

555 The analysis of the absorptions by climate zones approve that the absorption using the
 556 single average global atmosphere (AGA) profile has only 0.5 % difference to the sum of five
 557 different climate zones of the Earth. This means that the simulation using only one AGA
 558 profile is justified. The water content of a climate zone increases as the temperature
 559 becomes warmer. If the Earth would follow this humidity behavior, the water feedback would
 560 be positive and it would increase the warming impacts of other GH gases by 35 %.

561

562 The analysis of the period from 1979 to 2015 shows that the effects of water and other GH
 563 gases cannot explain the temperature trend. The warming impacts of GH gases (water
 564 feedback doubles the impacts of other GH gases) according to the IPCC model [24] are 44
 565 % higher than the observed temperature in 2015 when compared to the average
 566 temperature from 2000 to 2015. The same impacts calculated by Ollila's formula [6] for the
 567 radiative forcing of CO₂, shows that the difference varies from 0 to 0.45 °C during this period.
 568 The trend analysis shows that there is no water feedback during the three latest solar cycles.
 569 The conclusion is that the absolute water content can be kept constant in the long-term
 570 climate change analyses.

571

572 The detrended analysis shows very clearly that the short-term (1-2 years) CO₂ changes do
 573 not change the short-term absolute humidity values at all - there is no correlation. The culprit
 574 for the short-term changes is the ENSO event (El Niño and La Niña), which creates strong
 575 changes in the absolute water content. Usually this phenomenon is called positive water
 576 feedback but this term can be questioned in the ENSO events. When the temperature of the
 577 surface ocean increases, it increases evaporation and it gives rise to the water content in the
 578 atmosphere. The atmospheric TPW changes during ENSO events are the essential parts of
 579 the whole process and not actually separate feedback processes. The strong short-term
 580 global level changes of water amounts explain, why the El Niño and La Niña changes are so
 581 strong and why these regional phenomena have global effects after a 2-3 months' delay.

582

583 During the period from 1979 to 2015 there is only one short-term temperature change, which
584 is not due to the ENSO. That is the eruption of Mt. Pinatubo in 1991 leading to the sudden
585 global temperature drop of 0.5 °C, which gradually vanished by 1995. It is interesting to
586 analyze which kind of water feedback can be found if any. Soden et al. [35] reported that
587 there was a water positive feedback applying -0.75 mm TPW peak reduction as to the
588 NVAP-M trend [36] during the eruption. Ollila [37] found that it was impossible to draw any
589 conclusions based on the trend TWP values, because the two datasets had opposite trends
590 [26], [36]. The TPW trend in Fig. 4 is after NCEP/NCAR Reanalysis dataset and there is no
591 trend from 1991 to 1995 meaning no water feedback. Therefore, the conclusion of the
592 constant water content during the long-term temperature changes seems to be justified,
593 because TPW changes happen only during ENSO events. This result supports the climate
594 sensitivity (CS) calculations, where the absolute water amount has been assumed to be
595 constant, and which gives the CS value of 0.6 °C [6].
596

597 At the same time, there is an unknown force or forces, which create long-term temperature
598 changes like the strong warming from 1985 to 2000. These unexplained warming effects
599 vary between from 0 to 0.45 °C as noticed before. They could be cosmic forces. The
600 absolute water amount does not react to the long-term temperature changes (> 11 years).
601

602 The analyses of the GH gas impacts show that the impact of CO₂ is very nonlinear. The
603 effects of GH gases for the all-sky are: H₂O 79 %, CO₂ 13 %, O₃ 5 %, CH₄ & N₂O 1 % and
604 cloud 2 %. The cloud effort considers only the temporary (in average from 1 to 10 days)
605 cloudiness changes of the Earth. The long-term cloudiness change increases still have the
606 negative impact on the surface temperature (-0.1 °C / cloudiness-%). These results mean
607 that the all-sky values are close to clear sky values. The main reason is that the absorption
608 in the altitude of 1.6 km is already 93 % of the total absorption in the altitude of 120 km. In
609 these analyses the cloud base value has been 1.6 km and the cloud top value 4.0 km.
610

611 The effects of GH gases show that the warming effect of CO₂ is very nonlinear: in the GH
612 phenomenon waters strength to CO₂ is 6.2:1, and in the present climate it is 11.8:1. The total
613 absorption without CO₂ is 285.684 Wm⁻², which is very close to the absorption flux, if there is
614 only water in the atmosphere: 286.704 Wm⁻². This latter water absorption is possible only, if
615 the atmosphere can maintain the constant water amount 2.6 prcm of the present
616 atmosphere. The empirical data shows that this is the case of the relatively small long-term
617 changes of 0.5 °C. Whether this would happen in the case of the average temperature drop
618 of 4.3 °C, we have no physical evidence. Anyway, the climate system seems to prefer
619 maintaining the constant absolute water amount in the atmosphere rather than the constant
620 relative water amount (positive feedback) or negative feedback, which would mean the
621 constant greenhouse conditions.
622

623

624 REFERENCES

625

- 626 1. Gats, Inc. Spectral calculations tool: Available: <http://www.spectralcalc.com/info/help.php>
627 [2015](http://www.spectralcalc.com/info/help.php).
- 628 2. HITRAN, Harvard-Smithsonian Center for Astrophysics, The HITRAN (high-resolution
629 transmission molecular absorption) data base. Available:
630 <https://www.cfa.harvard.edu/hitran/>
- 631 3. Mlawer EJ, Payne VH, Moncet J-L, Delamere JS, Alvarado MJ, and Tobin DC.
632 Development and recent evaluation of the MT_CKD model of continuum absorption.
633 Philosophical transactions. Series A, Mathematical, physical, and engineering sciences.
634 2012;370:Jun 13:2520-56. doi:10.1098/rsta.2011.0295. 2012.

- 635 4. Michell JFB. The “greenhouse” effect and climate change. *Reviews of Geophysics*.
636 1989;27(1):115-139.
- 637 5. Kiehl JT and Trenberth KE. Earth’s annual global mean energy budget. *Bulletin of*
638 *American Meteorological Society*. 2009;90:311-323.
- 639 6. Ollila A. The potency of carbon dioxide (CO₂) as a greenhouse gas. *Development in*
640 *Earth Sciences*. 2014;2:20-30.
- 641 7. Schmidt GA, Ruedy RA, Miller RL, Lacis AA. Attribution of the present-day total
642 greenhouse effect. *Journal of Geophysical Research*. 2010;115:D20106.
643 doi:10.1029/2010JDO14287.
- 644 8. Clough SA, Iacono MJ. Line-by-line calculations of the atmospheric fluxes and cooling
645 rates 2. Application to carbon dioxide, ozone, methane, nitrous oxide and the
646 halocarbons. *Journal of Geophysical Research*. 1995;100:16519-16535.
- 647 9. Miskolczi FM, Mlynczak MG. The greenhouse effect and spectral decomposition of the
648 clear-sky terrestrial radiation. *Időjaras*. 2004;108:209-251.
- 649 10. Pierrehumbert RT. Infrared radiation and planetary temperature. *Physics Today*.
650 2011;64:33-38.
- 651 11. Ollila A. Analyses of IPCC’s warming calculations results. *Journal of Chemical, Biological*
652 *and Physical Sciences*. 2013;3:2912-2930.
- 653 12. Chambers J, Miller A, Morgan R, Officer B, Rayner M, Quirk T. Clearing air on climate.
654 *Energy & Environment*. 2010;21:632-639.
- 655 13. ISCCP. International Satellite Cloud Climatology Project. Cloud Data & Products.
656 Available: <http://isccp.giss.nasa.gov/products/onlineData.html>
- 657 14. Ollila A. Dynamics between clear, cloudy and all-sky conditions: cloud forcing effects.
658 *Journal of Chemical, Biological and Physical Sciences*. 2013,4:557-575.
- 659 15. Zhang Y, Rossow WB, Lacis AA, Oinas V, Mischenko MI. Calculation of radiative fluxes
660 from the surface to top of atmosphere based on ISCCP and other global data sets.:
661 Refinements of the radiative model and the input data. *Journal of Geophysical Research*.
662 2004:1149-1165.
- 663 16. Stine AR, Huybers P, Fung IY. Changes in the phase of the annual cycle of surface
664 temperature. *Nature*. 2009;457:435-441.
- 665 17. Kauppinen J, Heinonen JT, Malmi PJ. Major Portions in Climate Change: Physical
666 approach. *International Review of Physics*. 2011;5:260-270
- 667 18. Ollila A. Earth’s energy balance for clear, cloudy and all-sky conditions. *Development in*
668 *Earth Sciences*. 2013;1:1-9.
- 669 19. Ollila A, The roles of greenhouse gases in global warming. *Energy & Environment*.
670 2012;23:781-799.
- 671 20. Ollila A. Clear sky absorption of solar radiation by the average global atmosphere.
672 *Journal of Earth Sciences and Geotechnical Engineering*. 2015;5:19-34.
- 673 21. IPCC. Climate response to radiative forcing. IPCC Fourth Assessment Report (AR4),
674 The Physical Science Basis, Contribution of Working Group I to the Fourth Assessment
675 Report of the Intergovernmental Panel on Climate Change, Cambridge University Press,
676 Cambridge. 2007
- 677 22. Miskolczi F. The stable stationary value of the earth’s global average atmospheric
678 Planck-weighted greenhouse-gas optical thickness. *Energy & Environment*.
679 2010;21:243-262.
- 680 23. NOAA. Global CO₂ data base. Available:
681 ftp://afpp.cmdl.noaa.gov/products/trends/co2/co2_mm
- 682 24. IPCC. The Physical Science Basis. Working Group I Contribution to the IPCC Fifth
683 Assessment Report of the Intergovernmental Panel on Climate Change, Cambridge
684 University Press, Cambridge. 2013.
- 685 25. UAH MSU dataset. Available:
686 http://vortex.nsstc.uah.edu/data/msu/v6.0beta/tlt/uahncdc_lt_6.0beta5.txt
-

- 687 26. NVAP dataset. NCEP/NCAR Reanalysis. Available:
688 <http://www.esrl.noaa.gov/psd/data/timeseries/>
- 689 27. Ermakov V, Okhlopkov V, Stozhkov Y, Yu I. Influence of cosmic rays and cosmic dust on
690 the atmosphere and Earth's climate. *Bulletin of Russian Academy of Sciences: Physics*.
691 2009;73:434-436.
- 692 28. Scafetta N. Empirical evidence for a celestial origin of the climate oscillations and its
693 implications. *Journal of Atmospheric and Solar-Terrestrial Physics*. 2010;72:951-970.
- 694 29. Ollila A. Cosmic theories and greenhouse gases as explanations of global warming.
695 *Journal of Earth Sciences and Geotechnical Engineering*. 2015;5:27-43.
- 696 30. AGGI. The NOAA annual greenhouse index (AGGI). Available:
697 <http://www.esrl.noaa.gov/gmd/aggi/aggi.html>
- 698 31. Bellouin n, Boucher O, Haywood J, Shekar Reddy M. Global estimate of aerosol direct
699 radiative forcing from satellite measurement. *Nature*. 2003;438:1138-1141.
- 700 32. Chernykh IV, Alduchov OA, Eskridge RE. Trends in Low and High Cloud Boundaries
701 and Errors in Height Determination of Cloud Boundaries. *Bulletin of the American*
702 *Meteorological Society*. 2001;82:1941-1947.
- 703 33. Kokhanovsky AA, Rozanov VV, Lotz W, Bovensmann H, Burrows JP. Global cloud top
704 height and thermodynamic phase distributions as obtained by SCIAMACHY on
705 ENVISAT. *International Journal of Remote Sensing*. 2011;28:836-844.
- 706 34. Wang J, Rossow WB, Zhang Y. Cloud vertical structure and its variations from a 20-yr
707 global rawinsonde dataset. *Journal of Climate*. 2000;13:3041-3056.
- 708 35. Soden BJ, Wetherald RT, Stenchikov GL, Robock A. Global cooling after the eruption of
709 Mount Pinatubo: A test of climate feedback by water vapor. *Science*. 2002; 296:727-730.
- 710 36. Vonder Haar TH, Bytheway JL, Fortsyth JM. Weather and climate analyses using
711 improved global water vapor observations. *Geophysical Research Letters*.
712 2012;39:L16802.
- 713 37. Ollila A. Climate sensitivity parameter in the test of the Mount Pinatubo eruption.
714 *Physical Science International Journal*. 2016;9(4):1-14.
-